Numerical study of multiple injections under diesel engine conditions

M.A. Chishty[1], M. Bolla[1], E.R. Hawkes[1,2] and S. Kook[1]

[1]School of Mechanical and Manufacturing Engineering
University of New South Wales, Sydney 2052, Australia

[2]School of Photovoltaic & Renewable Energy Engineering
University of New South Wales, Sydney 2052, Australia

Abstract

In this study, numerical simulations of an *n*-dodecane spray flame in a constant volume chamber under diesel engine conditions – known as Spray A – with multiple-injections (0.5 / 0.5 dwell / 1.0 ms injection) have been carried out using the transported probability density function (TPDF) method in the Reynolds-averaged Navier-Stokes (RANS) framework. The realizable $k-\epsilon$ turbulence model was used to provide the turbulence information to the TPDF solver. The micro-mixing term was closed using the Interaction by Exchange with the Mean (IEM) model. The objective of the present study is to compare simulation results of soot and nitrogen oxide (NO) mass from a single and a double injection case with the same total injected fuel mass. The fuel-air mixing for the two different cases has been analysed in terms of mixture fraction probability density function (PDF) evolution. The results show that the ignition of the second injection is promoted by the high temperature gases originated from the combustion of the first injection with sufficiently low scalar dissipation rate. This advanced ignition of the second injection results in the increase of local temperature and equivalence ratio, resulting in an increase of the formed soot mass by a factor of four compared to the first injection. The double injection schedule reduced the NO mass in comparison with single injection and the net soot formation and oxidation rate where found to increase when fuel splitting was applied.

Introduction

New combustion modes have been established in the past few decades to enhance the air-fuel mixing and dilution i.e. Homogeneous Charge Compression Ignition as HCCI, Premixed Charge Compression Ignition as PCCI and Low-Temperature Combustion as LTC. However, these modes have disadvantages like emission of CO/Unburned Hydrocarbons (UHC) and also restrict the loads and engine speeds [3]. In recent years, researchers have introduced the multiple injections strategies to improve engine control, reduced combustion noise, and enhanced soot oxidation while maximising fuel economy [21, 27]. Also in conventional diesel engines, a small amount of fuel is introduced prior to the main injection to reduce the peak heat release rate and combustion noise [4, 28].

Multiple injections involve complex phenomenon and a strong coupling is expected between the combustion processes. Bruneaux and Maligne [3] investigated the basic mechanisms of interaction between two consecutive jets both in terms of mixing and combustion for a co-axial single-hole common rail diesel injector. They showed that the ignition of the second injection is promoted by the entrainment of high-temperature gases left over by the first injection. Similar findings have been observed by other researchers that, the ignition of the second injection was not governed by the ambient temperature but rather by the time when the jet reaches the high-temperature combustion products from the first injection with sufficiently low scalar dissipation rate [7,

18, 27]. The combustion of the second injection is in more fuel rich region and therefore, forming a higher concentration of polycyclic aromatic hydrocarbons (PAH) and soot compared to the first injection.

Numerical simulations can provide helpful insight into the complex interplay between processes involved with multiple injections. Splitting the fuel injection into pulses alters the combustion mode and the problem becomes a three-feed system with two fuel streams and an oxidizer stream. This brings along a considerable increase in complexity for typical combustion models which rely on a mixture fraction conditioning e.g. the Conditional Moment Closure (CMC) [2] and the Representative Interactive Flamelet (RIF) [10], the Flamelet Progress Variable (FPV) [1] and Flamelet Generated Manifold (FGM) [29]. In the context of RIF model formulation conditioned on two mixture fractions – denoted as 2D-RIF – has been introduced by Hasse et al. [14] and later successfully applied for metal diesel engines [11, 12]. An extended model for multiple injections has been proposed recently for CMC model in [13, 22] and applied for post-injection cases in optical heavy-duty diesel engines [20]. On the other hand, the transported probability density function (TPDF) method [15, 26] can handle the multiple injection cases without any modification because it does not assume that thermochemical states lie on a low-dimensional manifold (i.e. the mixture fraction). This method is used in this study because it has been successfully applied in the diesel engines for single-injection cases [5, 9, 24, 25] and recently for multiple injections in [7].

The scope of this work is to study numerically the effect of fuel injection splitting on the fuel-air mixing and on the formation of soot and NO. Two different injection schedules with the same total injected fuel have been considered: (1) single injection: 1.5 ms injection and (2) double injection: 0.5 / 0.5 dwell / 1.0 ms injection.

Numerical Methodology

In this study, the finite-volume based Fluent (version 14.5) commercial package was employed. The implementation of the TPDF model is the same as in our previous study; hence for full details, the reader is referred to our previous papers [5, 6, 8, 9, 23, 25]. Briefly, the joint composition PDF transport equations are solved using the Lagrangian Monte Carlo approach coupled with a time-dependent Reynolds-averaged $k-\epsilon$ turbulence model and the liquid spray is treated as a Lagrangian discrete phase model. The molecular mixing term is closed using the Interaction by Exchange with the Mean (IEM) mixing model with the model constant set to $C_\emptyset = 2.5$.

A 2D axisymmetric mesh having dimensions of 100×63 with a total number of cells of 2300 has been used. The convergence studies of mesh, time step size, the number of particles per cell and In-Situ Adaptive Tabulation (ISAT) error tolerance have

been conducted in previous studies [23]. A relatively compact reduced 53 species and 267 reactions *n*-dodecane chemical mechanism [30] has been employed in conjunction with the two-equation soot model by Leung et al. [17]. Both the chemical mechanism and soot model have been extensively validated in our previous work [6] at different ambient conditions. NO formation is modelled with the extended Zel'dovich mechanism [16].

The test case considered here is part of the Engine Combustion Network (ECN) and the nominal Spray A condition is considered, namely the ambient temperature, oxygen volume fraction and density 900 K, 15% and 22.8 kg/m^3, respectively. Liquid *n*-dodecane is injected at a pressure of 1500 bar. The single injection case with 1.5 ms injection duration is known as Spray A baseline, whereas the double injection case has been tailored in this study to represent a 'pilot+main' injection schedule. In this way, the total fuel mass injected is the same between the two cases allowing for a realistic comparison. Note that for this double injection test case no experimental data are available and the scope of this work is to perform a numerical analysis on the relative effect of splitting the fuel injection.

Results and Discussions

In this section, simulation results of single and double injections are compared in terms of soot mass and NO mass vs time. The fuel-air mixing of the two different injection schedules is compared by plotting the mixture fraction PDFs at selected times. Moreover, the temporal evolution of pollutant formation and oxidation are plotted for the single and double injection cases.

Soot and NO mass vs Time

Figure 1 shows the temporal evolution of simulated total soot and NO mass for the single (i.e. 1.5 ms in solid line) and double (i.e. 0.5 / 0.5 dwell / 1.0 ms in dashed line) injection cases at Spray A conditions. Soot is formed and subsequently oxidized after the end of injection due to oxidizer entrainment. For the double injection case two distinct peaks are depicted, corresponding to the two injection events. The timing of the peak soot mass is delayed by approximately 0.5 ms compared the end of the injection event, and this holds true for all three peaks portrayed in figure 1. This is due to the fluid and entrainment residence time needed from the injector to the soot region after the end of injection. The same effect is observed when considering that the soot mass as well as the NO mass is the same until around 0.9 ms although the end of the first injection was already at 0.5 ms. The soot maximal value for the double case is slightly higher and at the same time the net soot oxidation rate is also increased. Soot formation during the second injection is considerably larger than during the first injection. The main reason – apart the fact that the second injection releases more fuel – is that high-temperature combustion gases left from the first injection in the vicinity of the injector shortens the ignition delay of the second injection (roughly 0.2 vs 0.4 ms). Therefore, the local temperature and equivalence ratio of the second injection is higher leading to a significant increase in soot formation in comparison with the amount of soot formed in the first 0.5 ms injection. It has been noticed that the second injection produces four times more soot than the first injection, mainly due to the advanced ignition of second injection, which occurs near the liquid length where the local equivalence ratio is more fuel-rich [27].

The double injection schedule reduced the NO mass with only a minimal increase in the soot formation during the injection period i.e. 2 μg and did not extend the combustion duration. The possible reason for the reduction of NO emission is that the double injection retards the ignition timing while holding the soot emission at a low level.
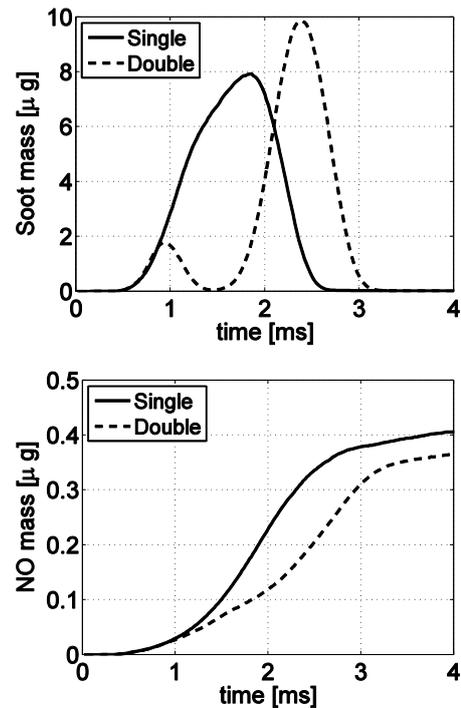
Figure 1: Comparison of soot mass (upper) and NO mass (lower) vs time for single and double injections (0.5 / 0.5 dwell / 1.0 ms) at Spray A ambient conditions

Mixture Fraction PDF

The overall mixing process is quantified by the evolution of the mixture fraction PDF within the entire domain. Three distinct time instants have been selected, namely during the injection, at the end of the injection and at the timing of the peak soot mass. The mixture fraction PDF is constructed from the notional particle data (200 particles per cell used here), and therefore also the subgrid scale mixture fluctuations have been included. Figure 2 depicts the mixture fraction PDF for the single (solid lines) and double (dashed lines) injection schedules. The solid blue vertical line shows the stoichiometric mixture fraction. t_S and t_D represent the time after start of injection for the single and double injection cases, respectively. The PDFs for both cases are compared at: t_S = 1.0 ms vs t_D = 1.5 ms, t_S = 1.5 ms vs t_D = 2.0 ms and t_S = 2.0 ms vs t_D = 2.5 ms. A shift of 0.5 ms between the two cases has been selected to have the same amount of fuel between the two cases at every time instant.

For the first time instant, when 2/3 of the fuel has been injected, there is a clear difference in the distribution between the two cases. The single injection case depicts a high probability in the fuel rich region, whereas for the split injection case, there is a clear shift of the mixture towards stoichiometric conditions. This is the result of the end of the first injection, which provokes an increase of the entrainment rate [19]. The observed leaning of the mixture is mostly related to the first 0.5 ms injected fuel. Interestingly, the tail of the PDF remains unaffected because the second fuel injection creates again rich mixture areas close to the injector.

At the second time instant – representing the respective end of injection – the mixture distribution of the single injection case is overall slightly leaner than before due to the spatial evolution of the jet, but the difference is minor. On the other hand, the double injection case becomes considerably richer due to the additional fuel injected and the distribution becomes more similar to the single case. This means that the relative effect of the pilot injection on the overall mixing is decreased with time. However,

at the end of injection, there are still some differences. Namely, the peak in the fuel lean region arising from the first injection is still visible.
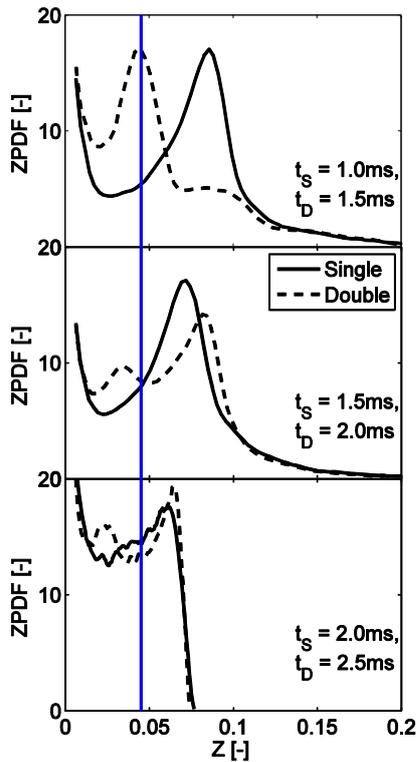
Figure 2: Mixture fraction PDF for the single (solid lines) and double injection (dashed lines) schedules at selected times. t_S and t_D represent the ASOI of single and double injection schedules, respectively. The solid blue line shows the stoichiometric mixture fraction.

After the end of injection, the maximal mixture fraction is considerably reduced for both cases due to mixing. Results between the two cases tend to merge. Note that the time after the end of injection is 0.5 ms for both cases. Also, the rate of injection ramp-down has been assumed to be the same between the cases. This is the reason for the very similar mixing behaviour. The relative differences in the fuel lean and rich regions between the cases observed in the intermediate time instant are still detectable.

Temporal Evolution of Pollutants

The relative differences in the partitioning of mixture fraction distribution have an influence on the propensity towards pollutant formation such as soot and NO. Figure 3 portrays the spatial distribution of soot-relevant quantities and NO for the single (upper half) and double injection case (bottom half) at the same three time instants as considered before. From left to right: computed mass fraction of acetylene (YC_2H_2), soot volume fraction (ppm), soot formation (1/s), soot oxidation (1/s), mass fraction of nitrogen oxide (YNO) and NO formation rate (1/s). The same scaling has been applied for all time instants and only half of the spray is illustrated due to the axisymmetric jet arrangement in a RANS context.

For the single injection case, the temporal evolution of YC_2H_2 and soot formation is steadily increasing during the injection period. Soot oxidation takes place at the periphery and in particular at the tip of the jet, where the mixing rate with the fresh oxidizer is high. After the end of injection, the leaning process reduces the C_2H_2 concentration and the formation rate of soot accordingly and the oxidation rate becomes more important. At the last time instant (peak soot mass time) these two effects

are counteracted and later the soot oxidation becomes more important and the soot mass is rapidly reduced within approximately 0.8 ms as shown in figure 1. The double injection case depicts an analogous process with the difference that the net formation and oxidation rate of soot is faster, where soot is oxidized with 0.6 ms.

At the first time instant, the double injection case has experienced a considerable leaning and this has oxidized the soot and has promoted more formation of NO because there is a larger amount of mixture at a slightly lean to stoichiometric conditions where most of the NO is formed. Also at the second time instant, there is more NO at the tip of the jet as the result of the leaner mixture. At later stage, the differences in NO are smaller and the total amount of NO formed is comparable between the two cases.

Conclusions

Numerical simulations of an n-dodecane spray flame – known as Spray A – with single (1.5 ms) and double injection (tS = 1.0 ms vs tD = 1.5 ms) schedules have been carried out using the TPDF method in the RANS framework. Particular attention has been paid to the formation of soot and NO. Results from a single and a double injection case having the same total amount of fuel injected have been compared to study the influence of fuel splitting on the soot and NO mass, fuel-air mixing and the flame structures of soot relevant quantities. Splitting of the fuel injection resulted initially into a leaner mixture where the soot is oxidized and more NO is formed, but the effect of the injection dwell on the mixture distribution is reduced at later stages, resulting in more similar distributions of different species as well as mixture fraction. The net soot formation and oxidation rate where found to increase when fuel splitting was applied.

Acknowledgments

References

[1] Bajaj, C., M. Ameen & J. Abraham, Evaluation of an Unsteady Flamelet Progress Variable Model for Autoignition and Flame Lift-Off in Diesel Jets, Combust. Sci. Technol. 185, 2013, 454-472.

[2] Bolla, M., D. Farrace, Y. M. Wright, K. Boulouchos & E. Mastorakos, Influence of turbulence–chemistry interaction for n-heptane spray combustion under diesel engine conditions with emphasis on soot formation and oxidation, Combust. Theor. Model. 18, 2014, 330-360.

[3] Bruneaux, G. & D. Maligne, Study of the Mixing and Combustion Processes of Consecutive Short Double Diesel Injections, SAE Int. J. Engines 2, 2009, 1151-1169.

[4] Chen, S. K. Simultaneous Reduction of NOx and Particulate Emissions by Using Multiple Injections in a Small Diesel Engine, SAE Technical Paper, 2000-01-3084, 2000.

[5] Chishty, M. A., M. Bolla, E. Hawkes, Y. Pei & S. Kook, Assessing the Importance of Radiative Heat Transfer for ECN Spray A Using the Transported PDF Method, SAE Int. J. Fuels Lubr. 9, 2016, 100-107.

[6] Chishty, M. A., M. Bolla, E. Hawkes, Y. Pei & S. Kook, Soot formation modelling for n-dodecane sprays using the transported PDF model, Combust. Flame 2016 (submitted).

[7] Chishty, M. A., M. Bolla, Y. Pei, E. R. Hawkes & S. Kook. A Numerical Study of 'Spray-A' with Multiple-Injections

Using the Transported PDF Method, in 10th Asia-Pacific Conference on Combustion Beijing, China, Paper No. 124, July 19-22, 2015.

[8] Chishty, M. A., M. Bolla, Y. Pei, E. R. Hawkes, S. Kook & T. Lu. Soot Formation Modelling of Spray-A Using a Transported PDF Approach, SAE Technical Paper, 2015-01-1849, 2015.

[9] Chishty, M. A., Y. Pei, E. R. Hawkes, M. Bolla & S. Kook. Investigation of the flame structure of Spray-A using the transported probability density function, in 19th Australasian Fluid Mechanics Conference Melbourne, Australia, Paper No. 432, 2014.

[10] D'Errico, G., T. Lucchini, F. Contino, M. Jangi & X. S. Bai, Comparison of well-mixed and multiple representative interactive flamelet approaches for diesel spray combustion modelling, Combust. Theor. Model. 18, 2014, 65-88.

[11] Doran, E. M., H. Pitsch & D. J. Cook. Multi-Dimensional Flamelet Modeling of Multiple Injection Diesel Engines, SAE Technical Paper, 2012-01-0133, 2012.

[12] Felsch, C., M. Gauding, C. Hasse, S. Vogel & N. Peters, An extended flamelet model for multiple injections in DI Diesel engines, Proc. Combust. Inst. 32, 2009, 2775-2783.

[13] Frapolli, N., M. Bolla, K. Boulouchos & Y. M. Wright. Simulations of In-Cylinder Processes in a Diesel Engine Operated with Post-Injections Using an Extended CMC Model, SAE Technical Paper, 2014-01-2571, 2014.

[14] Hasse, C. & N. Peters, A two mixture fraction flamelet model applied to split injections in a DI Diesel engine, Proc. Combust. Inst. 30, 2005, 2755-2762.

[15] Haworth, D. C., Progress in probability density function methods for turbulent reacting flows, Prog. Energy Combust. Sci. 36, 2010, 168-259.

[16] Lavoie, G. A., J. B. Heywood & J. C. Keck, Experimental and Theoretical Study of Nitric Oxide Formation in Internal Combustion Engines, Combust. Sci. Technol. 1, 1970, 313-326.

[17] Leung, K. M., R. P. Lindstedt & W. P. Jones, A simplified reaction mechanism for soot formation in nonpremixed flames, Combust. Flame 87, 1991, 289-305.

[18] Lim, J., S. Lee & K. Min, Combustion Modeling of Split Injection in HSDI Diesel Engines, Combust. Sci. Technol. 183, 2010, 180-201.

[19] Musculus, M. P. B. & K. Kattke, Entrainment Waves in Diesel Jets, SAE Int. J. Engines 2, 2009, 1170-1193.

[20] O'Connor, J. & M. Musculus, Effects of exhaust gas recirculation and load on soot in a heavy-duty optical diesel engine with close-coupled post injections for high-efficiency combustion phasing, Int. J. Engine Res. 2013.

[21] O'Connor, J. & M. Musculus, Post Injections for Soot Reduction in Diesel Engines: A Review of Current Understanding, SAE Int. J. Engines 6, 2013, 400-421.

[22] Pandurangi, S. S., N. Frapolli, M. Bolla, K. Boulouchos & Y. M. Wright, Influence of EGR on Post-Injection Effectiveness in a Heavy-Duty Diesel Engine Fuelled with n-Heptane, SAE Int. J. Engines 7, 2014, 1851-1862.

[23] Pei, Y., E. R. Hawkes & S. Kook, A Comprehensive Study of Effects of Mixing and Chemical Kinetic Models on Predictions of n-heptane Jet Ignitions with the PDF Method, Flow Turbulence Combust 91, 2013, 249-280.

[24] Pei, Y., E. R. Hawkes & S. Kook, Transported probability density function modelling of the vapour phase of an n-heptane jet at diesel engine conditions, Proc. Combust. Inst. 34, 2013, 3039-3047.

[25] Pei, Y., E. R. Hawkes, S. Kook, G. M. Goldin & T. Lu, Modelling n-dodecane spray and combustion with the transported probability density function method, Combust. Flame 162, 2015, 2006-2019.

[26] Pope, S. B., PDF methods for turbulent reactive flows, Prog. Energy Combust. Sci. 11, 1985, 119-192.

[27] Skeen, S., J. Manin & L. M. Pickett, Visualization of Ignition Processes in High-Pressure Sprays with Multiple Injections of n-Dodecane, SAE Int. J. Engines 8, 2015, 696-715.

[28] Tow, T. C., D. A. Pierpont & R. D. Reitz. Reducing Particulate and NOx Emissions by Using Multiple Injections in a Heavy Duty D.I. Diesel Engine, SAE Technical Paper, 940897, 1994.

[29] Wehrfritz, A., O. Kaario, V. Vuorinen & B. Somers, Large Eddy Simulation of n-dodecane spray flames using Flamelet Generated Manifolds, Combust. Flame 167, 2016, 113-131.

[30] Yao, T., Y. Pei, B.-J. Zhong, S. Som & T. Lu. A Hybrid mechanism for n-dodecane combustion with optimized low-temperature chemistry, in 9th U.S. National Combustion Meeting Internal combustion and gas turbine engines, Cincinnati, Ohio, Paper No. 1C02, May 17-20, 2015, 2015
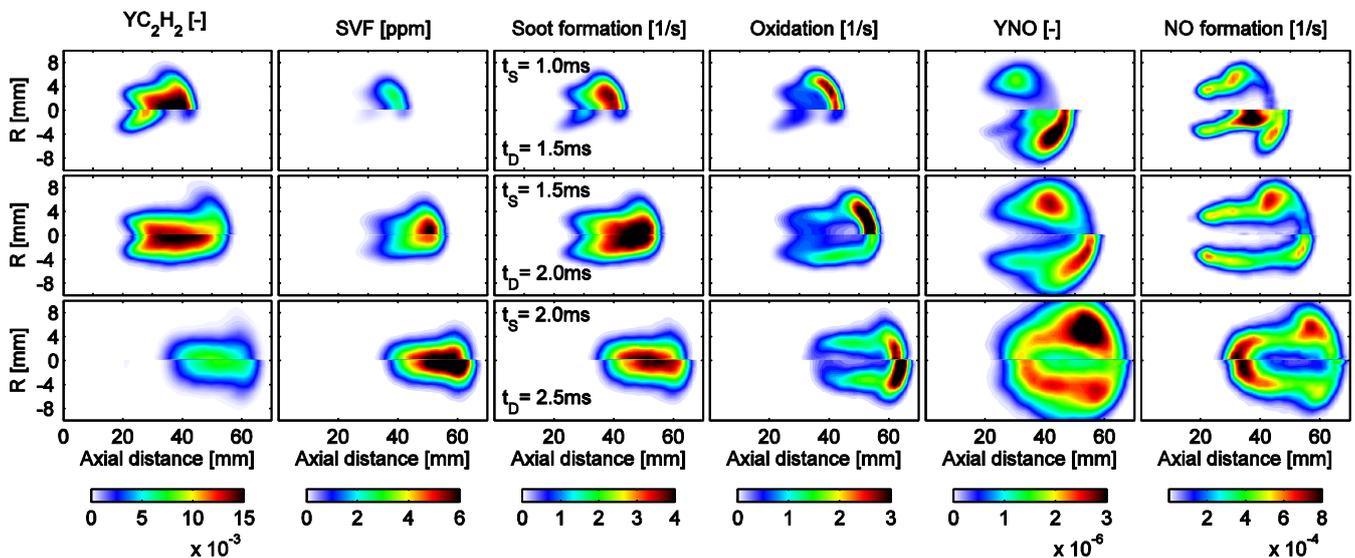
Figure 3: Comparison of spatial distributions of the single (upper half) and the double injection cases (lower half) at different time steps. From left to right: computed mass fraction of acetylene (YC_2H_2), soot volume fraction (ppm), soot formation (1/s), soot oxidation (1/s), mass fraction of nitrogen oxide (YNO) and NO formation rate (1/s), respectively.